Cancer Biol Med 2025. doi: 10.20892/j.issn.2095-3941.2025.0185

LETTER

Non-essential role of S100A9 in hematopoiesis in primary MPN and MDS mouse models

Qinglin Li[1]*, Xuezhen Ma[1]*, Zhaofeng Li[1]*, Xinshu Xie[1], Yating Lu[1], Hanqi Liu[1], Ailing Zou[1], Yexin Yang[1], Jie Ouyang[1], Shuqian Xu[2], Yang Mei[1]

[1]School of Biomedical Sciences, Hunan Provincial Key Laboratory of Animal Model and Molecular Medicine, Hunan University, Changsha 410082, China; [2]Department of Hematology, Qilu Hospital of Shandong University, Jinan 250012, China

S100 proteins govern cellular proliferation, differentiation, apoptosis, calcium homeostasis, energy metabolism, and inflammation. This heterodimeric calcium-binding protein, consisting of the S100A8 and S100A9 subunits, modulates myeloid cell development. S100A9 elevation has been found in myeloproliferative neoplasms (MPN), myelodysplastic syndrome (MDS), and acute myeloid leukemia (AML)[1-3]. Notably, transgenic mice with S100A9 overexpression develop myeloid dysplasia that closely mimics human MDS[2]. Haploinsufficiency in Rps14, a human del(5q) MDS-associated gene, leads to impaired erythroid differentiation and triggers overexpression of S100A8/S100A9[3]. However, whether endogenous S100A9 is essential for normal or pathological hematopoiesis *in vivo* is largely unknown.

To evaluate the roles of S100A9 in hematopoiesis, we analyzed *S100A9*$^{-/-}$ mice. Peripheral blood parameters and bone marrow (BM) or spleen (SP) cellularity analysis showed scarcely any differences between WT and S100A9 null mice (**Figures S1 and S2**). We therefore induced stress hematopoiesis by treating the mice with 5-fluorouracil (5-Fu) and phenylhydrazine (PHZ). Unexpectedly, S100A9 loss had minimal effects on the mice during hematopoietic recovery (**Figures S3 and S4**).

We next asked whether S100A9 might play roles in hematological malignant conditions, such as MPN and MDS. We first crossed *S100A9*$^{-/-}$ mice with MPN mice (*JAK2*$^{V617F/+}$*Vav-Cre*)—a model closely resembling human polycythemia vera. The *JAK2*^{V617F} mutation attenuated survival regardless of the presence of S100A9 expression (**Figure 1A**). Moreover, the splenomegaly in *JAK2*^{V617F} mutant mice was not alleviated by S100A9 deletion (**Figure 1B**). BM and SP cellularity did not differ between *JAK2*^{V617F}*Vav-Cre* and *JAK2*^{V617F}*S100A9*$^{-/-}$*Vav-Cre* mice (**Figure 1C**). Erythrocytosis promoted by *JAK2*^{V617F} mutation was not alleviated by S100A9 depletion, despite a decline in platelet counts observed in *JAK2*^{V617F}*S100A9*$^{-/-}$*Vav-Cre* mice (**Figure 1D and Figure S5A–T**). This outcome, combined with the previously described role of S100A9 in facilitating the formation of procoagulant platelets through GPIbα[4], underscores S100A9's role in promoting thrombopoiesis. Subsequently, we conducted lineage analysis through flow cytometry assays. The *JAK2*^{V617F} mutant mice exhibited aberrant elevations in both the proportions and cell counts of TER119^{+} erythroid cells in the BM and SP (**Figure 1D and Figure S5U**). However, the deletion of S100A9 in the presence of *JAK2*^{V617F} mutation only slightly ameliorated the absolute number of erythroid cells in the BM but not the SP (**Figure 1D**), and the percentages remained unchanged (**Figure S5U**). Likewise, myeloid and lymphoid cells in BM or SP showed no differences between *JAK2*^{V617F} mutant mice and JAK2/S100A9 double-mutant mice (**Figure 1D and Figure S5V**). These results suggest that S100A9 does not substantially contribute to the pathogenesis of *JAK2*$^{V617F/+}$-driven polycythemia. A prior study has indicated that the overexpression of S100A9, triggered by the *Srsf2*^{P95H} mutation, hindered polycythemia in *JAK2*$^{V617F/+}$ mice[5]. Together, these results indicate that

*These authors contributed equally to this work.
Correspondence to: Shuqian Xu and Yang Mei
E-mail: shuqian.xu@email.sdu.edu.cn and yanmei@hnu.edu.cn
ORCID ID: https://orcid.org/0000-0001-7071-8550 and https://orcid.org/0000-0002-0432-2897
Received April 13, 2025; accepted June 3, 2025.
Available at www.cancerbiomed.org
©2025 The Authors. Creative Commons Attribution-NonCommercial 4.0 International License

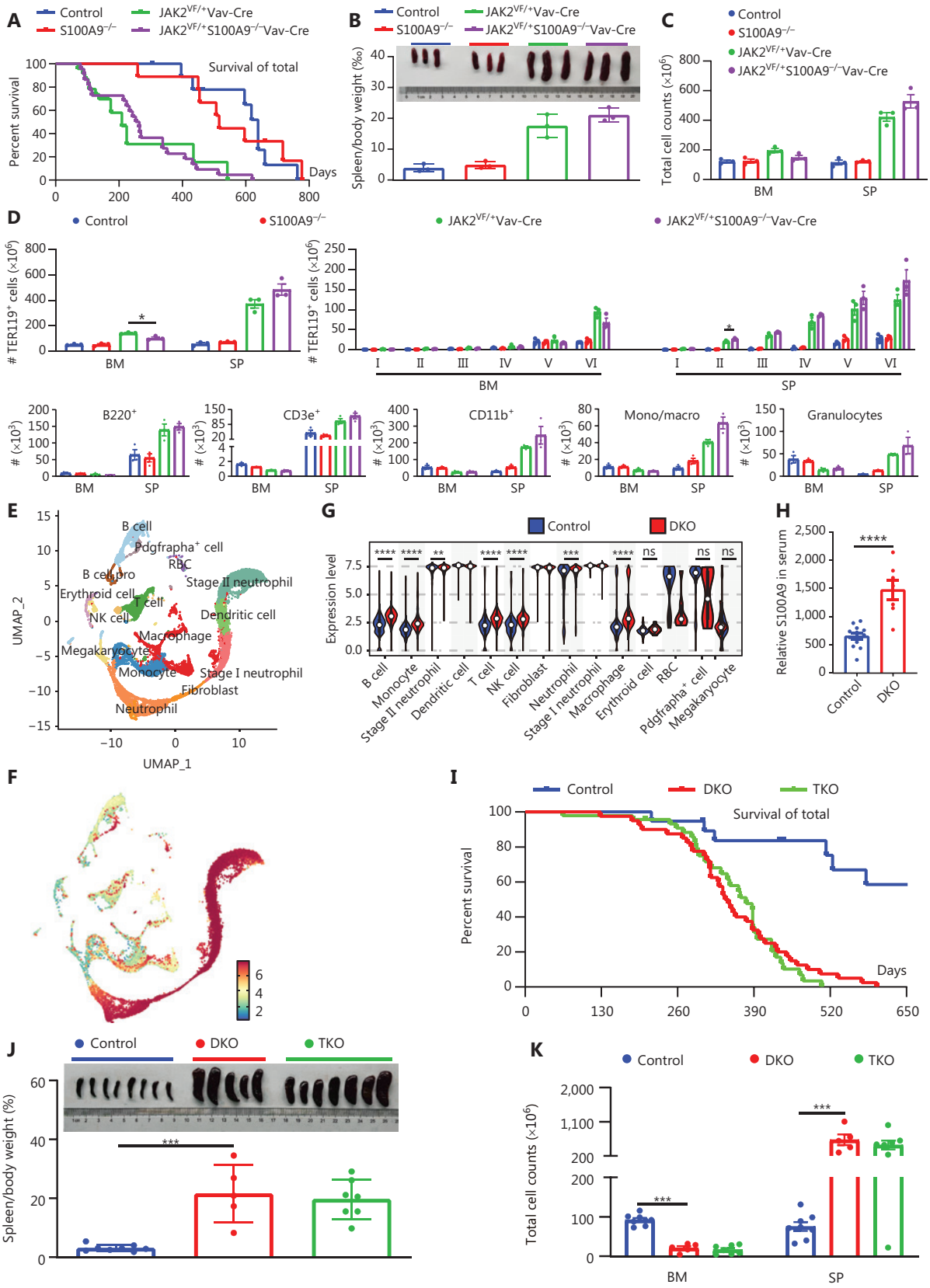


Figure 1 Continued

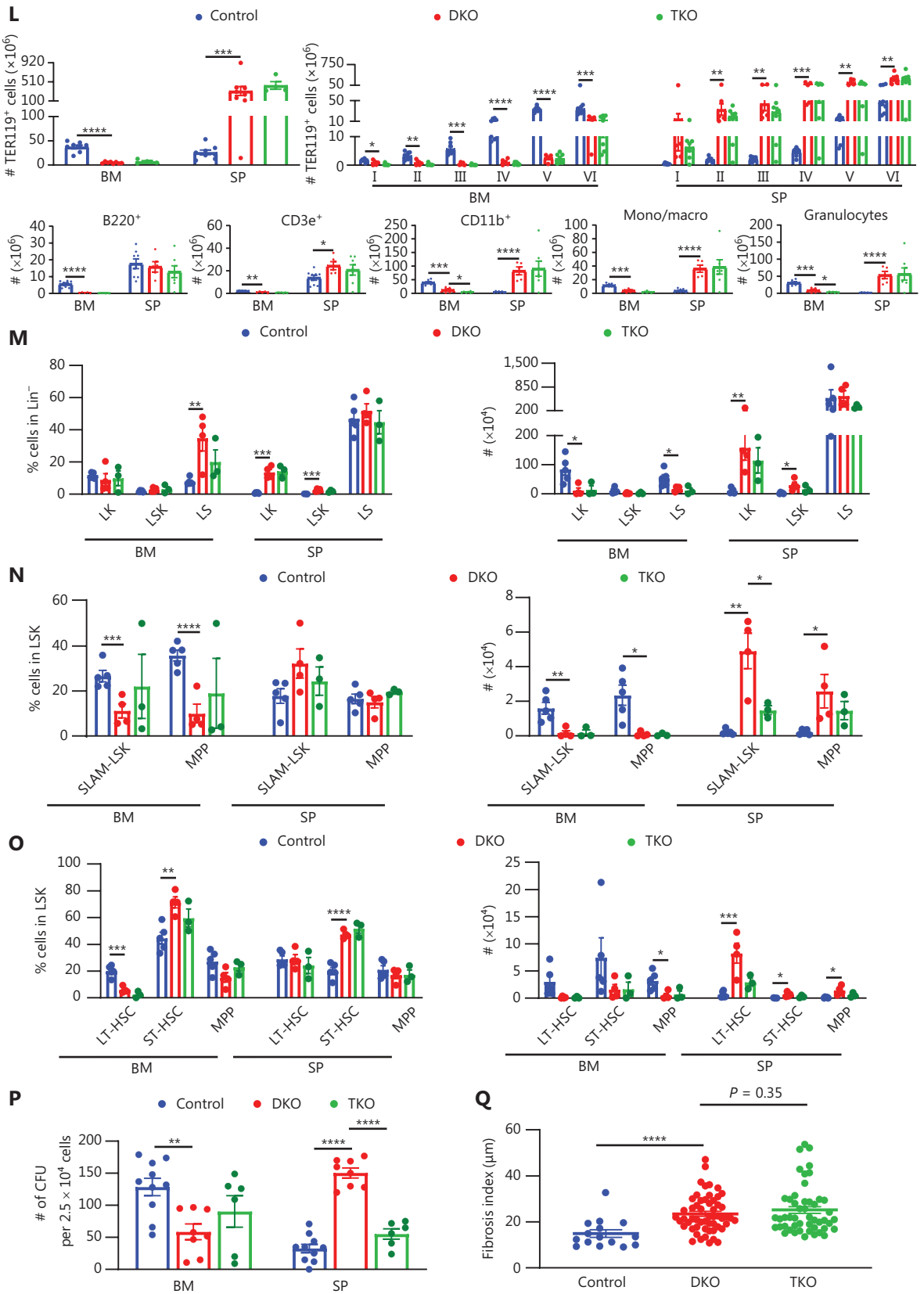


Figure 1 Continued

Figure 1 S100A9 is not required for hematopoietic dysfunction in the *JAK2*^{V617F} mutant MPN and age-related MDS mouse model. (A) Kaplan–Meier survival curve showing the survival of the indicated mice. Control, *n* = 10; *S100A9*$^{-/-}$, *n* = 9; *JAK2*$^{VF/+}$*Vav-Cre*, *n* = 23; *JAK2*$^{VF/+}$*S100A9*$^{-/-}$*Vav-Cre*, *n* = 22. (B) Quantitative analyses of spleen weight *vs.* body weight. *n* = 3 per group. (C) Absolute cell counts in the BM and SP from the indicated mice. *n* = 3 per group. (D) Flow cytometry analysis of TER119$^+$ erythroid, lymphoid, and myeloid cells in the BM and SP. Top, quantification of absolute counts of TER119$^+$ erythroid cells and various differentiation stages of erythroid cells. I–VI represent proerythroblasts (ProE), basophilic erythroblasts (BasoE), polychromatic erythroblasts (PolyE), orthochromatic erythroblasts (OrthoE), reticulocytes (Ret), and red blood cells (RBCs). *n* = 3 per group. Bottom, absolute counts of lymphoid and myeloid cells. B cells, B220$^+$; T cells, CD3e$^+$; myeloid cells, CD11b$^+$; monocytes/macrophages, Ly6G$^-$CD11b$^+$; granulocytes, Ly6G$^+$CD11b$^+$. *n* = 3 per group. (E) Merged UMAP plots showing the distribution and overlap of annotated cell populations from the BM of aged (12- to 14-month-old) control and DKO mice. (F) As in I, except that the S100A9 expression pattern is illustrated on merged UMAP plots. (G) Violin plots showing S100A9 expression levels across the indicated cell populations. (H) Relative serum S100A9 levels, determined by multiplex ELISA. Control, *n* = 12; DKO, *n* = 7. (I) Kaplan–Meier survival analysis assessing the effects of combined S100A9 deletion in *Diaph1*$^{-/-}$ *Mir146*$^{-/-}$ mice. Control, *n* = 17; DKO, *n* = 40; TKO, *n* = 46. (J) Quantitative analysis of spleen weight normalized to body weight. (K) Absolute cell numbers in the BM and SP. (L) Flow cytometry analysis of TER119$^+$ erythroid, lymphoid, and myeloid cells in the BM and SP. Top, quantification of absolute counts of TER119$^+$ erythroid cells and various differentiation stages of erythroid cells. I, ProE; II, BasoE; III, PolyE; IV, OrthoE; V, reticulocytes; and VI, RBCs. Bottom, absolute counts of lymphoid and myeloid cells. B cells, B220$^+$; T cells, CD3e$^+$; myeloid cells, CD11b$^+$; monocytes/macrophages, Ly6G$^-$CD11b$^+$; granulocytes, Ly6G$^+$CD11b$^+$. Control, *n* = 8; DKO, *n* = 5; TKO, *n* = 7. (M) Percentages (left) and absolute cell counts (right) of LK (Lin$^-$c-Kit$^+$Sca1$^-$), LSK (Lin$^-$c-Kit$^+$Sca1$^+$), and LS (Lin$^-$c-Kit$^-$Sca1$^+$) cells in the BM lineage negative cells (Lin$^-$) of the indicated mice. (N) SLAM-LSK (CD150$^+$CD48$^-$LSK) and MPP (CD150$^-$CD48$^-$LSK) were gated from LSK cells of the indicated mice; frequency (left) and cell count (right) are shown. (O) Analysis of LT-HSC (CD135$^+$CD34$^-$LSK), ST-HSC (CD135$^-$CD34$^-$LSK), and MPP (CD135$^-$CD34$^+$LSK), similarly to N. (P) Colony formation assays of bone marrow mononuclear cells isolated from the indicated mice. Colonies were scored 14 days post-plating. (Q) Fibrosis in the sternum from the indicated mice, assessed through reticulin staining, with the fibrotic index quantified by fiber length measurement. DKO, Diaph1$^{-/-}$ Mir146$^{-/-}$; TKO, Diaph1$^{-/-}$Mir146$^{-/-}$ S100A9$^{-/-}$. Control, *n* = 8; DKO, *n* = 5; TKO, *n* = 7 in H–J; control, *n* = 5; DKO, *n* = 4; TKO, *n* = 3 in J–L; control, *n* = 10; DKO, *n* = 8; TKO, *n* = 6 in P; quantified colony numbers in Q were as follows: control, *n* = 15; DKO, *n* = 55; TKO, *n* = 49. All data are shown as mean ± SEM. All *P* values were calculated with 2-tailed unpaired Student's t-tests, except in G, in which the Wilcoxon Rank-Sum test was used. **P* < 0.05, ***P* < 0.01, ****P* < 0.001, *****P* < 0.0001.

activation, rather than deletion, of S100A9 might be a suitable approach for MPN therapy.

We have previously reported that mice with dual deficiency in mDia1 and MiR-146a (DKO mice) show age-related anemia and ineffective erythropoiesis mimicking human MDS[6]. Subsequent single-cell RNA-sequencing analysis of BM nucleated cells revealed enriched S100A9 expression in neutrophils, dendritic cells, fibroblasts, and macrophages (**Figure 1E–G**)[7]. Specifically, S100A9 was aberrantly overexpressed in B cells, monocytes, stage II neutrophils, T cells, NK cells, neutrophils, and macrophages in DKO mice (**Figure 1G**). Moreover, serum S100A9 was significantly higher in DKO mice than controls (**Figure 1H**). These results collectively suggested that S100A9 might potentially contribute to MDS pathogenesis. Therefore, we crossed the DKO mice with *S100A9*$^{-/-}$ mice to generate *Diaph1*$^{-/-}$*Mir146*$^{-/-}$*S100A9*$^{-/-}$ triple knockout (TKO) mice to interrogate the roles of S100A9 in MDS pathogenesis. Firstly, the survival curves were similar between DKO and TKO mice during aging (**Figure 1I**). Accordingly, peripheral blood parameters showed minimal differences between DKO and TKO mice, except for neutrophil counts (**Figure S6A–T**). An enlarged SP and extramedullary erythropoiesis were consistently observed in DKO mice and were not alleviated by S100A9 ablation (**Figure 1J–K**). Moreover, the loss of BM cellularity in DKO mice was not ameliorated by S100A9 deletion (**Figure 1K**). The impaired BM erythropoiesis in DKO animals, as evidenced by the disappearance of varied developmental stages of erythroid cells, was not recovered or ameliorated after S100A9 loss in TKO mice (**Figure 1L and Figure S6U**). We observed similar patterns for lymphoid cells (**Figure 1L and Figure S6V**, B220$^+$ and CD3e$^+$). Notably, in agreement with the diminished peripheral neutrophil counts in TKO mice (**Figure S6R**), myelopoiesis was further impaired in DKO mice after S100A9 inactivation (**Figure 1L and Figure S6V**, CD11b$^+$, monocytes/macrophages, and granulocytes). This observation might be attributable to S100A9-mediated modulation of CD11b expression on neutrophils under pathological conditions such as inflammation[8]. Secondly, our analysis of the hematopoietic stem progenitor cells (HSPCs) in the BM and SP revealed that the common progenitors (LK, CMP, and GMP), multipotent progenitors (MPP), and hematopoietic stem cells (HSCs), including long-term HSCs (LT-HSCs) and SLAM-LSK were depleted in the BM but markedly accumulated in the SP in aged DKO mice (**Figure 1M–O and Figure S7A–D**). Intriguingly, although S100A9 deletion did

not restore BM HSPC levels, it substantially decreased splenic HSPC accumulation in DKO mice (**Figure 1N**). This finding was further validated through *in vitro* colony-forming assays in mononuclear cells (**Figure 1P and Figure S7E–H**). Our findings suggested that S100A9 is critical for either HSPC migration from the BM into the SP or the expansion of splenic HSPCs in the context of MDS. Thirdly, aged DKO mice exhibited fibrosis, as evidenced by reticulin staining in BM sections. However, the inactivation of S100A9 scarcely ameliorated the fibrotic conditions in DKO mice (**Figure 1Q and Figure S7I**).

Perspectives

In summary, our genetic studies demonstrated that loss of S100A9 expression contributes minimally to pathophysiological hematopoiesis in primary MDS and MPN mouse models. S100A9 typically forms both homodimers and heterodimers with S100A8. Emerging evidence highlights the non-redundant roles of S100 proteins in hematological malignancies. For example, the inactivation of S100A8 expression has been found to rescue the impaired erythroid differentiation in Rps14-haploinsufficient HSPCs[3]. S100A8 sustains the immature phenotype in AML, and its deletion impedes MLL-AF9-induced AML progression *in vivo*[9,10]. Whereas recombinant S100A9 enhances AML cell differentiation and prolongs survival in leukemic animal models[9], silencing of S100A9 paradoxically decreases AML cell viability and proliferation[11]. In addition, enhancer of zeste homolog 2 (EZH2) inhibition in high-risk MDS induces S100A9 overexpression, thereby activating pyroptosis[12]. Diminished S100A9 expression mediates leukemic transformation induced by SETD2 deficiency in an MDS mouse model (NUP98-HOXD13 transgenic mice), and exogenously supplied recombinant S100A9 decreases the expansion of HSPCs from these compound mice, as demonstrated in colony-forming unit (CFU) assays *in vitro*[13]. Whether S100A8 might compensate for S100A9 loss warrants further study. Further investigations should also be conducted to determine whether S100A8 play a more central role than S100A9 in the pathogenesis of MDS or MPN *in vivo*.

Acknowledgments

We thank all the authors for their input and discussions regarding this work. We appreciate the donation of *S100A9*$^{-/-}$ mice from Jiahe Xie at Gannan Medical University.

Grant support

This work was supported by grants from the National Natural Science Foundation of China (Grant Nos. 82170160 and 32000604), the Provincial Natural Science Foundation of Hunan (Grant Nos. 2021JJ30163 and 2022JJ20021), the Changsha Municipal Natural Science Foundation (Grant No. kq2007053), and the Global Research Award from American Society of Hematology to Y. M. This work was also partially supported by the National Natural Science Foundation of China (Grant No. 82470145) and Mount Taishan Scholar Young Expert of Shandong Province (Grant No. tsqn202103167) to S. X.

Conflict of interest statement

No potential conflicts of interest are disclosed.

Author contributions

Conceived and designed the analysis: Qinglin Li, Zhaofeng Li, Xuezhen Ma, Shuqian Xu, Yang Mei.
Collected the data: Qinglin Li, Zhaofeng Li, Xuezhen Ma, Xinshu Xie, Yating Lu, Hanqi Liu, Ailing Zou, Yexin Yang, Jie Ouyang.
Contributed data or analysis tools: Qinglin Li, Zhaofeng Li, Xinshu Xie, Shuqian Xu, Yang Mei.
Performed the analysis: Qinglin Li, Zhaofeng Li, Yang Mei.
Wrote the paper: Qinglin Li, Shuqian Xu, Yang Mei.

Data availability statement

The data generated in this study are available upon reasonable request from the corresponding authors.

References

1. Leimkühler NB, Gleitz HFE, Ronghui L, Snoeren IAM, Fuchs SNR, Nagai JS, et al. Heterogeneous bone-marrow stromal progenitors drive myelofibrosis via a druggable alarmin axis. Cell Stem Cell. 2021; 28: 637-52.
2. Chen X, Eksioglu EA, Zhou J, Zhang L, Djeu J, Fortenbery N, et al. Induction of myelodysplasia by myeloid-derived suppressor cells. J Clin Invest. 2013; 123: 4595-611.
3. Schneider RK, Schenone M, Ferreira MV, Kramann R, Joyce CE, Hartigan C, et al. Rps14 haploinsufficiency causes a block in erythroid differentiation mediated by S100A8 and S100A9. Nat Med. 2016; 22: 288-97.

4. Colicchia M, Schrottmaier WC, Perrella G, Reyat JS, Begum J, Slater A, et al. S100A8/A9 drives the formation of procoagulant platelets through GPIbα. Blood. 2022; 140: 2626-43.
5. Yang Y, Abbas S, Sayem MA, Dutta A, Mohi G. SRSF2 mutation reduces polycythemia and impairs hematopoietic progenitor functions in JAK2V617F-driven myeloproliferative neoplasm. Blood Cancer J. 2023; 13: 171.
6. Mei Y, Zhao B, Basiorka AA, Yang J, Cao L, Zhang J, et al. Age-related inflammatory bone marrow microenvironment induces ineffective erythropoiesis mimicking del(5q) MDS. Leukemia. 2018; 32: 1023-33.
7. Mei Y, Ren KH, Liu YJ, Ma A, Xia ZJ, Han X, et al. Bone marrow-confined IL-6 signaling mediates the progression of myelodysplastic syndromes to acute myeloid leukemia. J Clin Invest. 2022; 132: e152673.
8. Scott NR, Swanson RV, Al-Hammadi N, Domingo-Gonzalez R, Rangel-Moreno J, Kriel BA, et al. S100A8/A9 regulates CD11b expression and neutrophil recruitment during chronic tuberculosis. J Clin Invest. 2020; 130: 3098-112.
9. Laouedj M, Tardif MR, Gil L, Raquil MA, Lachhab A, Pelletier M, et al. S100A9 induces differentiation of acute myeloid leukemia cells through TLR4. Blood. 2017; 129: 1980-90.
10. Nicolas E, Ramus C, Berthier S, Arlotto M, Bouamrani A, Lefebvre C, et al. Expression of S100A8 in leukemic cells predicts poor survival in de novo AML patients. Leukemia. 2011; 25: 57-65.
11. Fan R, Satilmis H, Vandewalle N, Verheye E, De Bruyne E, Menu E, et al. Targeting S100A9 protein affects mTOR-ER stress signaling and increases venetoclax sensitivity in Acute Myeloid Leukemia. Blood Cancer J. 2023; 13: 188.
12. Zhang Q, Luo Y, Ye L, Wang Y, Wang L, Yang W, et al. EZH2 inhibition induces pyroptosis via RHA-mediated S100A9 overexpression in myelodysplastic syndromes. Exp Hematol Oncol. 2025; 14: 9.
13. Chen BY, Song J, Hu CL, Chen SB, Zhang Q, Xu CH, et al. SETD2 deficiency accelerates MDS-associated leukemogenesis via S100a9 in NHD13 mice and predicts poor prognosis in MDS. Blood. 2020; 135: 2271-85.

Cite this article as: Li Q, Ma X, Li Z, Xie X, Lu Y, Liu H, et al. Non-essential role of S100A9 in hematopoiesis in primary MPN and MDS mouse models. Cancer Biol Med. 2025; 22: 806-811. doi: 10.20892/j.issn.2095-3941.2025.0185